Reduction of α-Keto Acids by Low-Valent Metal Ions. 2. Reaction of Aqueous Vanadous Ion with Pyruvic and Phenylglyoxylic Acids

J. Konstantatos,* E. Vrachnou-Astra, N. Katsaros, and D. Katakis[1]

Contribution from the Chemistry Department, Nuclear Research Center "Demokritos", Aghia Paraskevi Attikis, Athens, Greece. *Received August 10, 1979*

Abstract: Vanadium(II) ion reacts with pyruvic and phenylglyoxylic acids in aqueous acidic solutions. The first stage of both reactions corresponds to a rapid equilibrium between the V(II) ion and the organic molecule. The second stage corresponds to the reduction of the organic compound. The products of the reduction are dimethyltartaric acid and diphenyltartaric acid, respectively. During the reduction steps V(II) ion is oxidized to V(III) ion. The overall stoichiometry for both reactions is 1:1. The kinetics of the redox steps were studied spectrophotometrically, and mainly by the stopped-flow technique. Reaction mechanisms are proposed for both reactions in which radical formation during the redox steps accounts for the products in both cases.

Introduction

In the reduction of pyruvic acid by chromous ion the stoichiometry of the overall reaction is 2:1 and the product lactic acid.[2] The rate-determining step is the hydro to keto conversion of the organic acid. As a result the kinetics of the redox step itself could not be studied.

In this paper we report on the corresponding reaction with vanadous ion. The change from a d^4 (chromous) to a d^3 (vanadous) ion results in a profound change in the stoichiometry (1:1), the product (dimethyltartaric acid),[3] and the rate law. The kinetics in this case are determined by the redox reaction, which is slow compared to the establishment of equilibrium between the hydro and the keto form of pyruvic acid. The redox steps are also slow compared to the entrance of pyruvate into the inner coordination sphere of V_{aq}^{2+}.

It can be argued that the important events which lead to the differences between chromous and vanadous ions are localized on the metal ions, on the organic substrate, or on both. Independently, however, of any mechanistic interpretation that might be given, and considering that the two metal ions differ only by one electron and react with the same oxidant, the empirical differences themselves can be characterized as very impressive indeed.

The investigation is extended to another keto acid, phenylglyoxylic acid.

Our general objective is contributing in the understanding of the ways low-valent metal ions interact with free ligands. The study of the reduction of keto acids by a variety of metal ions is part of this general project, but is also interesting by itself on two grounds: first, because it provides a new perspective in looking at the corresponding electron transfer reactions between metal ions, with pyruvato as a bridging ligand;[4] second because of the biological importance of the reduction of pyruvic acid.[5]

For pyruvic acid (**1**) we use the abbreviation pyr, for phenylglyoxylic acid (**2**) pgl, for dimethyltartaric acid (**3**) dmt, and for diphenyltartaric acid (**4**) dpt.

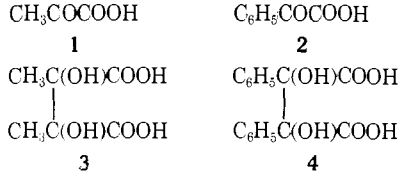

Experimental Section

Materials. Triply distilled water was used in all experiments. Solutions of vanadium(II) perchlorate were prepared by electrolytic reduction of pervanadic acid. The latter was prepared by treating V_2O_5 with H_2O_2 in acidic solution.[6] The concentrations of V_{aq}^{2+} and V_{aq}^{3+} were determined spectrophotometrically from the absorbances at 860 nm, where V_{aq}^{2+} shows a maximum (ϵ 2.8 M^{-1} cm^{-1}), and at 400 nm, where V_{aq}^{3+} shows a maximum (ϵ 8.12 M^{-1} cm^{-1}). The absorptivity for V_{aq}^{2+} at 400 nm is 0.82 M^{-1} cm^{-1}.

Sodium pyruvate was supplied by Merck and phenylglyoxylic acid by Fluka. Both reagents were stored at ~0 °C.

Stoichiometry. The stoichiometry of the overall reaction was determined in excess of V_{aq}^{2+} over ligand and vice versa. In the first case the excess of V_{aq}^{2+}, after the reaction was completed, was determined spectrophotometrically. In the second, the unreacted pyr and pgl were determined polarographically on a Metrohm A.G. Herisau rapid polarograph. Pyr was determined in a citrate-phosphate buffer of pH 3.95 after the product V_{aq}^{3+} was removed by ion exchange. Pgl could be measured in the presence of V_{aq}^{3+} because their cathodic waves are well separated.

Chromatographic Separations. The vanadium ions were removed from the reaction mixtures on a column of Dowex 50WX2 cation exchange resin.

Reaction Products. The reaction was performed by mixing air-free argon-saturated solutions. In the case of pyr, after its reaction with V^{2+} was completed, the reaction mixture was passed through the Dowex 50W column. The eluates contained the organic product. dmt was isolated by precipitation with excess $BaCl_2$ in neutral solution. In the case of pgl after the reaction is completed and the reaction mixture is allowed to stand for some time a precipitate appears to form. This precipitate was identified as diphenyltartaric acid. The remainder of the product was recovered from the reaction mixture by extraction with ether. The products were identified by elemental analysis, H^1 NMR, and mass spectrometry.

Kinetic Measurements. The kinetics were followed spectrophotometrically by observing the change in absorbance due to the oxidation of V(II) to V(III), in the region from 400 to 420 nm. Depending on the conditions, the rates of the redox reactions were followed either on an Applied Photophysics Ltd. stopped-flow apparatus or on a Cary 14 spectrophotometer.

Results

Reaction Stages, Products, and Stoichiometry. The first stage for both reactions is too fast to be followed under any of the experimental conditions we have tried and it appears as an increase in the absorbance within a time scale shorter than the dead time of the stopped-flow instrument. Figures 1 and 2 show typical oscilloscope traces for the two reactions, V_{aq}^{2+} with pyr and V_{aq}^{2+} with pgl, respectively. For the second reaction a third stage is also observed following the redox stage. This third stage is manifested by a decrease in the absorbance and under suitable conditions it is well time resolved from the redox stage.

For concentration ratios [V(II)]/[pyr] smaller than 2:1 the

0002-7863/80/1502-3035$01.00/0

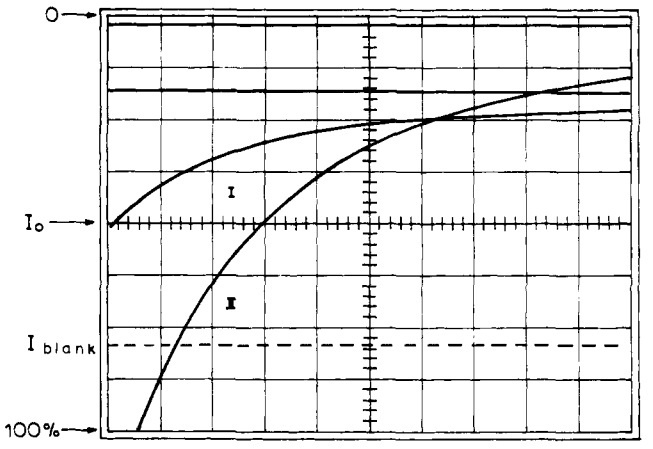

Figure 1. Stopped-flow traces for the reaction of V(II) with pyruvic acid. [V(II)] = 0.0375 M, [pyr] = 0.50 M, [$HClO_4$] = 1.0 M, temperature 25 °C. Ordinate corresponds to transmittance. For trace I (0.2 V/div) transmittance limits 0 and 100% are shown in the diagram. Trace II was taken under the same conditions as trace I but at four times higher sensitivity. Abscissa shows the time (200 ms/div). Horizontal solid lines correspond to "infinite" time. Dotted line (at 0.2 V/div) corresponds to the sum of the absorbances of the two reagents. The decrease in transmittance from I_{blank} to I_0 corresponds to the rapid establishment of equilibrium 1.

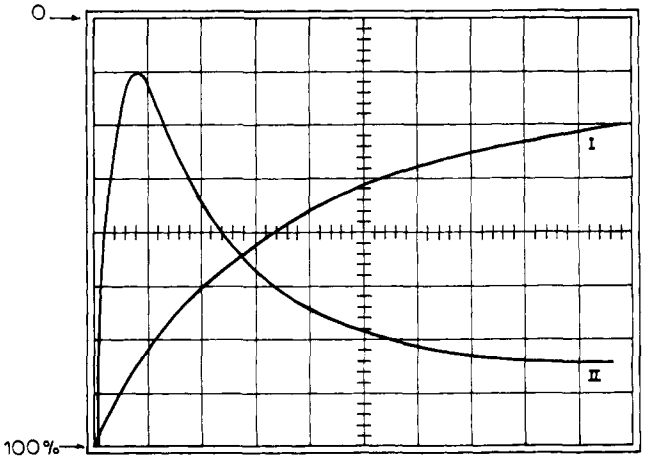

Figure 2. Stopped-flow traces for the reaction of V(II) with phenylglyoxylic acid. [V(II)] = 0.020 M, [pgl] = 0.10 M, [$HClO_4$] = 1.0 M, temperature 25 °C. Ordinate gives voltage values which are proportional to transmittance. Full scale corresponds to 1.6 V. Trace I corresponds to stage II, and trace II corresponds to stage III. For trace I: 0.05 V/div, 100 ms/div. For trace II: 0.02 V/div, 2 s/div.

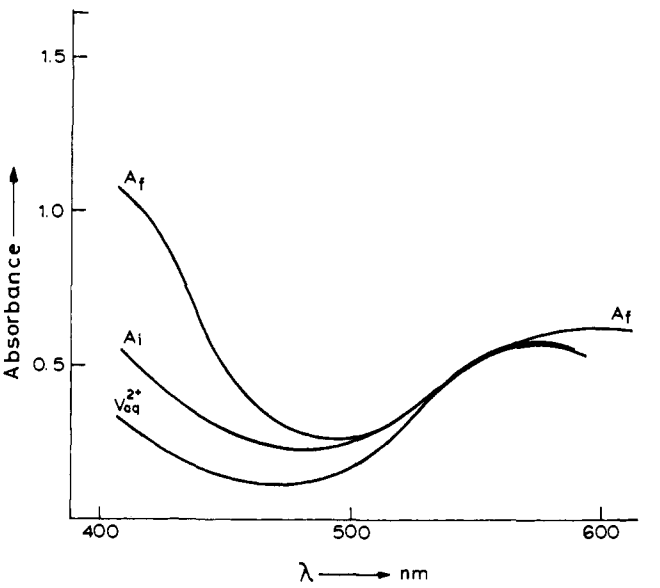

Figure 3. Reaction of aqueous V(II) ion with pyruvic acid. Absorbances at "zero time", A_i, and at "infinite time", A_f, are shown as a function of wavelength. These results were obtained in the stopped-flow instrument for $[V^{2+}]_0$ = 0.05 M, $[pyr]_0$ = 0.50 M, and [$HClO_4$] = 1.0 M. The spectrum of V_{aq}^{2+} is also included for comparison. $[V_{aq}^{2+}]$ = 0.05 M.

Table I. Overall Stoichiometry for the Reactions of V_{aq}^{2+} with pyr and pgl

composition of reaction mixtures				mmol of V_{aq}^{2+} consumed per mmol of organic acid
$[V_{aq}^{2+}]$ M	pyr M	pgl M	$HClO_4$	
0.077	0.005		2.0	1.21
0.077	0.005		1.0	1.19
0.077	0.005		0.3	1.20
0.059	0.005		1.0	1.07
0.079	0.079		2.0	1.01
0.079	0.079		1.0	0.99
0.065	0.065		0.3	1.0
0.065	0.130		1.0	0.98
0.065	0.200		1.0	1.01
0.059		0.015	3.0	0.99
0.059		0.015	0.5	1.00
0.059		0.029	3.0	0.98
0.059		0.029	0.5	0.97
0.018		0.018	1.0	1.01
0.018		0.036	1.0	0.99
0.018		0.054	1.0	1.00

stoichiometry in the reaction between V_{aq}^{2+} and pyruvic acid is 1:1 (Table I) and the product is dimethyltartaric acid. For larger ratios the stoichiometry becomes larger than 1:1 and lactic acid forms as a minor product. In the reaction of V_{aq}^{2+} with phenylglyoxylic acid the stoichiometry is 1:1 for all concentrations studied (Table I) and the product diphenyltartaric acid.

It may be instructive to mention here that equilibrium between V_{aq}^{2+} and lactic acid is too fast to observe in our stopped-flow instrument ($k > 10^2\ M^{-1}\ s^{-1}$). On the contrary, the overall reaction between V_{aq}^{2+} and tartaric acid is quite slow ($k \sim 10^{-2}\ M^{-1}\ s^{-1}$). In fact it is noteworthy that tartaric acid reacts even with the labile V_{aq}^{3+} slowly enough to be seen on the stopped-flow instrument, whereas complex formation reactions of V_{aq}^{3+} with pyruvic and lactic acids are too fast for stopped-flow.

Half-wave potentials of pyruvic and phenylglyoxylic acids were determined polarographically in 0.1 M HCl solutions, at 10^{-3} M concentrations; $E_{1/2}$ = −0.62 and −0.37 V for pyr and pgl, respectively, indicating that pgl is a better oxidant than pyr.

Spectrophotometric Investigation. A. Reaction of V_{aq}^{2+} with Pyruvic Acid. In order to identify the absorbing species the absorbances at "zero time", A_i, and at "infinite time", A_f, were monitored in the stopped-flow instrument as a function of wavelength from 400 to 640 nm. The results for $[V_{aq}^{2+}]_0 = 5.0 \times 10^{-2}$ M, $[pyr]_0$ = 0.5 M, and [$HClO_4$] = 1.0 M are given in Figure 3, where the spectrum of V_{aq}^{2+} is also recorded, under the same total V_{aq}^{2+} concentration, for comparison. It is clear from this figure that spectrum A_i can be attributed to V(II) species. The higher absorbance at shorter wavelengths is due to the tail of the charge-transfer band of the V(II)-pyr complex. Spectrum A_f is essentially the spectrum of V_{aq}^{3+}. A_i was found to increase with increasing ligand concentration at a fixed wavelength, 420 nm. At this wavelength the tail of the charge-transfer band gives substantial absorbance values, whereas the absorption of pyr for concentrations as high as 1.25 M is small and easily accounted for.

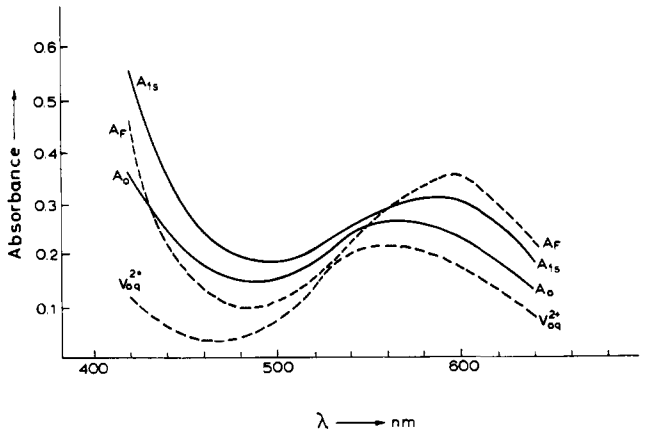

Figure 4. Reaction of aqueous V(II) ion with phenylglyoxylic acid. Absorbances at "zero time", A_0, time of 1 s, A_{1s}, and of "infinite time", A_f, are shown as a function of wavelength. These results were obtained in the stopped-flow instrument for $[V^{2+}]_0 = 0.02$ M, $[pgl]_0 = 0.10$ M, and $[HClO_4] = 1.0$ M. The spectrum of V_{aq}^{2+} is also included for comparison.

B. Reaction of V_{aq}^{2+} with pgl. For this reaction monitoring of the change of the absorbance vs. time revealed, in addition to two stages analogous to the previous reaction, a third stage. This stage was manifested by a decrease in the absorbance and under the appropriate conditions it can be time resolved from stage II. An oscillogram showing all the stages for this reaction is given in Figure 2. Absorbances A_i, A_{1s}, and A_f corresponding to "zero time", time of 1 s, and "infinite" time, were monitored in the stopped-flow instrument against wavelength in the region 400–650 nm. These spectra together with the spectrum of V_{aq}^{2+} are shown in Figure 4, for $[V_{aq}^{2+}]_0 = 0.02$ M, $[pgl]_0 = 0.10$ M, and $[HClO_4] = 1.0$ M. Under these conditions, time lapse of 1 s approximately corresponds to completion of stage II.

Formation Constants and Absorptivities of the V(II) Complexes. The formation constants and the absorptivities of the complexes formed upon mixing were estimated by determining the apparent absorptivity at different total ligand concentrations which were in large excess over the metal ion. For relatively unstable one to one complexes the apparent absorptivity ϵ is given[7] by the formula

$$\bar{\epsilon} = (\epsilon_0 + \epsilon_1 K[L])/(1 + K[L])$$

where ϵ_0 and ϵ_1 are the absorptivities at 420 nm of V_{aq}^{2+} and the complex, respectively, K is the formation constant, and [L] is the total ligand concentration, which for large excess of ligand over metal ion can be taken approximately equal to the free ligand concentration. On rearrangement the formula becomes

$$\frac{1}{\bar{\epsilon} - \epsilon_0} = \frac{1}{\epsilon_1 - \epsilon_0} + \frac{1}{K(\epsilon_1 - \epsilon_0)[L]}$$

Figure 5 includes plots of this equation for the two acids investigated, obtained in 1.0 M $HClO_4$ solutions. The results obtained from the slopes and intercepts of Figure 5 are $\epsilon_1 = 31 \pm 3$ (at 420 nm) and $K = 0.20 \pm 0.03$ for pyr; $\epsilon_1' \simeq 35$ (at 420 nm) and $K' \simeq 4$ for pgl.

For the case of pgl the values for ϵ_1' and K' are approximate (the error may be as high as 50%) owing to the limited range of pgl concentrations. The equilibrium constant for the reaction

$$V_{aq}^{3+} + pyr \rightleftarrows V^{3+}\text{-pyr}$$

was also measured; $K'' = 0.75$. The absorptivity for the V^{3+}-pyr at 420 nm is $\epsilon_1'' = 11.6$.

Kinetics. A. Reaction of V_{aq}^{2+} with pyr. The rate of the second stage for this reaction was followed for concentrations of V_{aq}^{2+} and hydrogen ion in excess over pyr. The experimental data for a range of initial concentrations of V_{aq}^{2+} are given in Table IIA. The entries below V_{aq}^{2+} in this table have not been corrected for partial conversion to the pyruvato complex. On the basis of the formula

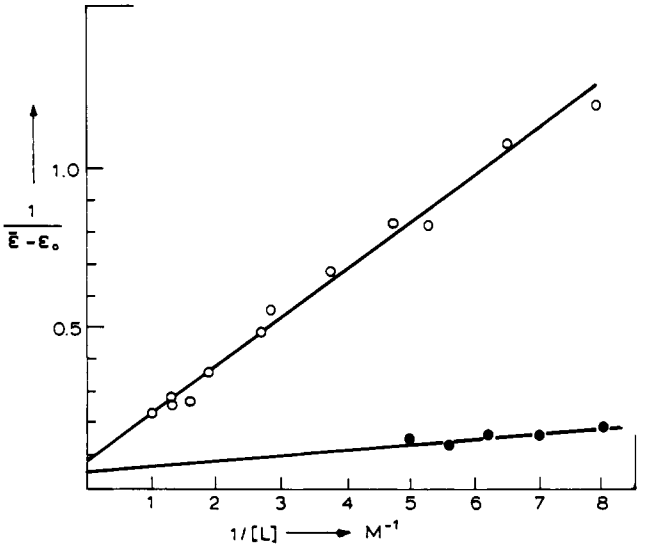

Figure 5. Plots of $1/(\bar{\epsilon} - \epsilon_0)$ vs. $1/L$. Open circles correspond to pyr. Closed circles correspond to pgl. For the second case data are limited owing to the limited range of pgl concentrations.

Table II. Kinetic Data for the Reduction of Pyruvic Acid by V(II)[a]

A				
$[V_{aq}^{2+}] \times 10^2$, M	[pyr] × 10^2, M	$[HClO_4]$, M	k''_{obsd}	$k''_{obsd}/[V^{2+}]$
15.7	0.50	1.0	1.46	9.30
15.7	0.50	1.0	1.43	9.10
12.0	0.50	1.0	0.89	7.40
9.0	0.50	1.0	0.61	6.75
7.9	0.50	1.0	0.43	5.50
7.7	0.50	1.0	0.45	5.82
6.4	0.50	1.0	0.32	5.00
5.2	0.50	1.0	0.23	4.50
5.1	0.50	1.0	0.26	5.10
3.9	0.50	1.0	0.14	3.69
3.8	0.50	1.0	0.16	4.15

B				
$[V_{aq}^{2+}] \times 10^2$, M	[pyr], M	$[HClO_4]$, M	$S^{(exptl)}$, Figure 7	$S^{(calcd)}$, $k_i[pyr]^2/2.3$
5.5	0.750	2.5	0.677	0.590 ± 0.090
5.3	0.750	1.0	0.620	0.590 ± 0.090
5.3	0.625	1.0	0.440	0.410 ± 0.060
7.5	0.500	1.0	0.267	0.260 ± 0.040
7.5	0.500	1.0	0.235	0.260 ± 0.040[b]
5.5	0.375	1.0	0.157	0.147 ± 0.020
5.5	0.260	1.0	0.074	0.070 ± 0.010
5.5	0.200	1.0	0.048	0.042 ± 0.007

C				
$[V_{aq}^{2+}] \times 10^3$, M	[pyr] × 10, M	$[HClO_4]$, M	$k^1_{obsd} \times 10^2$	$k_i = k_{obsd}/[pyr]^2$
2.5	0.75	1.0	1.190	2.12
5.0	0.50	1.0	0.560	2.23
2.5	0.38	1.0	0.320	2.16
2.5	0.25	1.0	0.146	2.34
2.5	0.25	1.0	0.134	2.14

[a] Temperature 26 °C; λ 420 (A, B), 400 nm (C). [b] 1.0 M $NaClO_4$ present in the V_{aq}^{2+} solution.

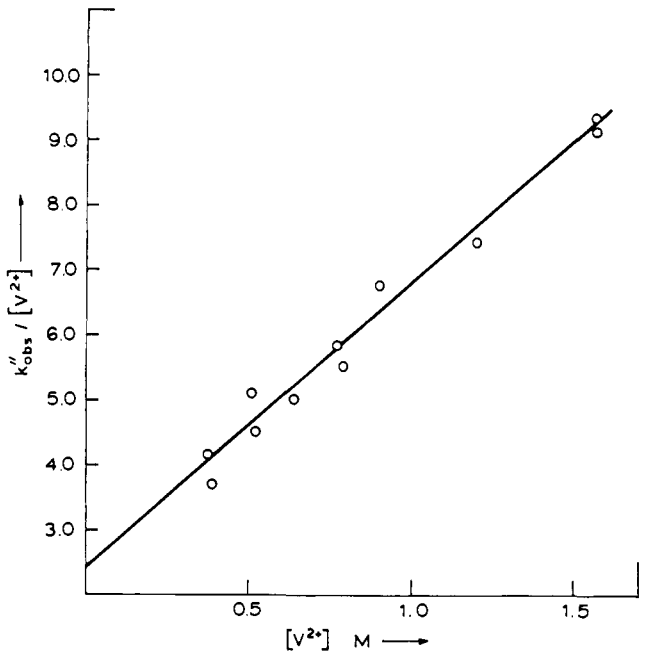

Figure 6. Plot of $k''_{obsd}[V^{2+}]$ vs. $[V^{2+}]$ at 1.0 M $HClO_4$ and 26 °C. From the slope and intercept of this plot k_{ii} and k_i are calculated respectively: $k_i = 2.4 \pm 0.4\ M^{-2}\ s^{-1}$ and $k_{ii} = 43 \pm 4\ M^{-3}\ s^{-1}$.

$$[V^{3+}] = \frac{\frac{A}{l} - \frac{[V^{2+}]_0(\epsilon_0 + \epsilon_1 K[pyr])}{1 + K[pyr]}}{\frac{\epsilon_0'' + \epsilon_1 K''[pyr]}{1 + K''[pyr]} - \frac{\epsilon_0 + \epsilon_1 K[pyr]}{1 + K[pyr]}} \qquad (a)$$

we estimate that even in excess pyruvic acid the correction does not amount to more than 2%. In the above formula A is the absorbance, l is the length of the cell, $[V^{2+}]_0$ is the initial concentration of vanadous, ϵ_0, ϵ_1, ϵ_0'', and ϵ_1'' are the absorptivities of V_{aq}^{2+}, V^{II}-pyr, V_{aq}^{3+}, and V^{III}-pyr, respectively. At 420 nm $\epsilon_0 = 0.61$, $\epsilon_1 = 31$, $\epsilon_0'' = 6.7$, and $\epsilon_1'' = 11.6$. K and K'' are the formation constants for V^{II}-pyr and V^{III}-pyr, respectively (0.20 and 0.75).

For all runs in Table II second-order kinetics were always observed suggesting a second-order dependence of the rate upon [pyr]. The variation of k''_{obsd} with initial concentration of V_{aq}^{2+} gave an order with respect to $[V^{2+}]$ between the values 1 and 2.

The rate of the same reaction was also followed for concentrations of pyr and hydrogen ion in excess over V_{aq}^{2+}. The kinetic data in this case do not fit either first- or second-order kinetics in accordance with the previous observation.

The above observations suggested that the reaction follows two parallel paths, one obeying first-order kinetics and the other second-order kinetics with respect to V_{aq}^{2+} concentration. The following rate law was considered:

$$R = \{k_i[V^{2+}] + k_{ii}[V^{2+}]^2\}[pyr]^2 \qquad (I)$$

and it was further tested.

i. On the basis of eq I, k''_{obsd} from Table IA must be identified with

$$k_i[V^{2+}] + k_{ii}[V^{2+}]^2$$

and plots of $k''_{obsd}[V^{2+}]$ vs. $[V^{2+}]$ should be linear. Such a linear plot is shown in Figure 6. From this plot k_i and k_{ii} were calculated:

$$k_i = 2.4 \pm 0.4\ M^{-2}\ s^{-1}\ k_{ii} = 43 \pm 4\ M^{-3}\ s^{-1}$$

ii. Rate eq I under conditions of large excess of pyr over V_{aq}^{2+} can be integrated to

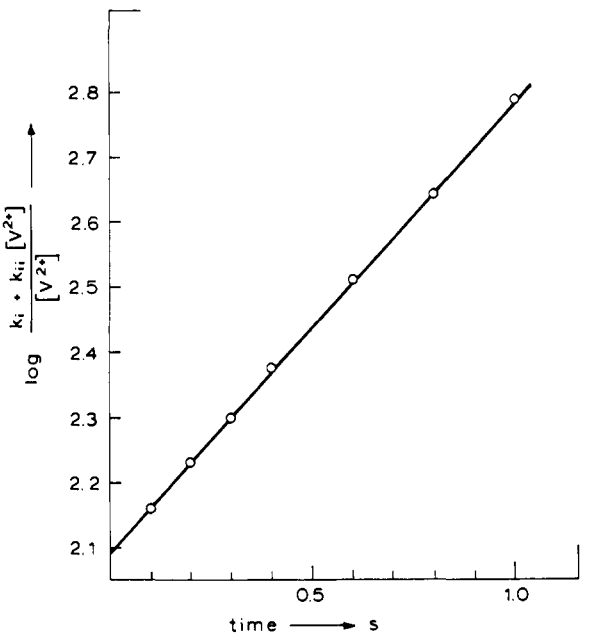

Figure 7. A plot of eq II. [pyr] = 0.75 M, $[V^{2+}]$ = 0.053 M, and $[HClO_4]$ = 1.0 M. Slope $S = 0.62$.

$$\log \frac{k_i + k_{ii}[V^{2+}]}{[V^{2+}]} = k_i A t/2.303 + C \qquad (II)$$

where $A = [pyr]^2$ and C = integration constant.

Knowledge of k_i and k_{ii} allows plotting of eq II. Indeed experimental data obtained under conditions of excess pyr over V_{aq}^{2+} fit eq II and give values for the slope $S = k_i[pyr]^2/2.303$. A typical plot of eq II is shown in Figure 7. Values of the slopes for such plots are given together with the corresponding calculated values in Table IIB. The good agreement of the two sets of values gives a good support of rate law I.

iii. Equation I, under conditions of excess pyr over V_{aq}^{2+} and sufficiently low concentrations of both reactants, may be approximated to

$$R = k_i[V^{2+}][pyr]^2 \qquad (III)$$

and first-order kinetics with respect to V^{2+} must be observed. Because of the low rate of the reaction under these conditions, kinetic runs in this case were carried out in a conventional spectrophotometer (Cary 14). With this instrument, optical cells up to 10 cm long can be used in comparison with the 2-cm long (fixed length) observation chamber of the stopped-flow instrument. The kinetic data are given in Table IIC. The observed first-order rate constants are in good agreement with the calculated $k_i[pyr]^2$ values.

The rate of the reaction was independent of the H^+ concentration for the range 0.5–2.5 M $HClO_4$.

A study of the temperature dependence of k''_{obsd} in the temperature range from 16 to 55 °C showed no appreciable change for this constant. The value of k''_{obsd} at 55 °C was less than 10% higher than its value at 16 °C. Since k''_{obsd} is really a composite constant, the effect of temperature cannot be used in a straightforward manner to derive activation parameters, but it can still be useful in drawing some qualitative conclusions (vide infra).

B. Reaction of V_{aq}^{2+} with pgl. The rate of this reaction was higher than the pyruvic acid reaction and its kinetics were studied entirely in the stopped-flow apparatus. The kinetic data for this reaction are shown in Table III. The entries under $[V_{aq}^{2+}]$ have not been corrected for complexation, because we were unable to measure the formation constant for V^{III}-pgl.

The data in Table III are not extensive because overlap of stages II and III could be avoided only under a rather

Table III. Kinetic Data for the Reduction of Phenylglyoxylic Acid by V(II), Temperature 25 °C

$[V_{aq}^{2+}]$, M	[pgl], M	$[HClO_4]$, M	k_{obsd} (stage II)	k'_{obsd} (stage III)
0.020	0.100	0.2	2.30	0.075
0.020	0.100	0.2	2.24	0.073[a]
0.020	0.100	0.5	2.16	0.064
0.020	0.100	1.0	2.70	0.280
0.020	0.100	1.0	2.65	0.220
0.020	0.100	2.0	4.03	0.340
0.100	0.010	1.0	2.60	0.460
0.009	0.100	1.0	2.17	0.330
0.009	0.050	1.0	1.30	0.145
0.018	0.200	1.0	5.70	1.040
0.090	0.010	1.0	2.67	0.260[b]
0.090	0.005	1.0	2.94	0.280[b]
0.045	0.005	1.0	1.47	0.190[b]

[a] $NaClO_4$ (0.8 M) was added. [b] For these runs temperature was 27 °C. $k_{obsd}^{(2)} = k_{2a}K_{1a}$. For $K_{1a} = 4$, $k_{2a} = 6.5 \pm 0.7$ s^{-1}

narrow and carefully selected range of experimental conditions. In addition to this an upper limit in pgl concentration (0.2 M pgl in 1.0 M $HClO_4$) was found to exist in perchloric acid solutions. Although pgl is very soluble in water, its solubility is greatly reduced in acid solutions. In spite of the fact that these data are not extensive, however, they clearly show that for stage II the rate law is

$$R = k^{(2)}_{obsd}[V^{2+}][pgl] \qquad (IV)$$

and that $k^{(2)}_{obsd}$ is independent of the hydrogen ion concentration for the range from 0.2 to 2.0 M $HClO_4$. $k^{(2)}_{obsd} = 26 \pm 3$ M^{-1} s^{-1}. For stage III first-order kinetics with respect to the change of the absorbance were observed. Although the exact dependence of the observed rate constant upon reactant concentration cannot be assessed, a rise of it with increase in concentration of any of the reactants, V_{aq}^{2+}, pgl, and hydrogen ion, is observed.

Discussion

For the reaction of V_{aq}^{2+} with pyr the following mechanism is proposed:

$$V_{aq}^{2+} + pyr \overset{fast}{\rightleftharpoons} \{V\text{-}pyr\}^{2+} \qquad (1)$$

$$\{V\text{-}pyr\}^{2+} + pyr \overset{fast}{\rightleftharpoons} \{V(pyr)_2\}^{2+} \qquad (2)$$

$$\{V(pyr)_2\}^{2+} \xrightarrow{slow} V^{3+} + pyr + \dot{p}yr \qquad (3)$$

$$2\dot{p}yr \xrightarrow{fast} dmt \qquad (4)$$

$$\{V\text{-}pyr\}^{2+} + \{V\text{-}pyr\}^{2+} \xrightarrow{slow} 2V^{3+} + dmt \qquad (5)$$

where $\dot{p}yr$ is a free radical. V_{aq}^{3+} is in equilibrium with the complexes formed with the organic product and excess pyruvic acid. On the basis of this mechanism the observed rate constants k_i and k_{ii} are identified with $k_3K_1K_2$ and $k_5K_1^2$, respectively. The linearity of the plots in Figure 5 suggests that equilibrium (1) is the main contributor to the absorbance values observed upon mixing. This is to be expected if the ratio, K_1/K_2, for the two successive stability constants for a six-coordinated complex ion is taken to be approximately 20. If one identifies K_1 with K and uses its value obtained from Figure 5, one can calculate the approximate values for the constants $k_3 = 1.2 \times 10^3$ s^{-1} and $k_5 = 1.07 \times 10^3$ M^{-1} s^{-1} of the elementary reactions (3) and (5).

On the basis of the rate law alone it is impossible to decide whether the second pyruvate in reaction 2 enters the first coordination sphere of V(II) or not. Hence, $V(pyr)_2$ must be considered as an empirical formula representing a real (inner sphere) complex or simply an outer-sphere association of the type V-pyr···pyr or pyr-V-OH_2···pyr. It can be suggested, however, that the interaction of the second pyruvate with V-pyr is quite strong, since it clearly facilitates the removal of the electron from the metal center by providing additional driving force. In this context, an elementary, yet important, remark should be made.

The slow step in a reaction sequence is not necessarily the reaction having the smaller rate constant, but rather the reaction having the slower rate. In our case, the rate constant for substitution is of the order of 10^2 M^{-1} s^{-1}, whereas the rate constant for the bimolecular electron transfer step is of the order of 10^3 M^{-1} s^{-1}. Yet rate determining is the latter. For a solution containing initially $[V_{aq}^{2+}] = 0.157$ M, [pyr] = 0.005 M the initial rate for substitution reaction (1) is $R_1 \simeq 7.85 \times 10^{-2}$ M s^{-1}, for the redox reaction (5) $R_5 \simeq 2.3 \times 10^{-5}$ M s^{-1}. Similarly, for a solution having initially $[V_{aq}^{2+}] = 0.01$ M, [pyr] = 0.50 M, $R_1 \simeq 0.5$ M s^{-1}, $R_3 \simeq 0.05$ M s^{-1}. We therefore observe redox reactions, whereas in the corresponding reaction[4] of V_{aq}^{2+} with the pyruvato complex of Co(III) the rate is determined by the substitution step.

The temperature insensitivity of k''_{obsd} suggests exothermic forward reactions for equilibria 1 and 2.

The detection, in excess V_{aq}^{2+}, of lactic acid and the corresponding change of the stoichiometry (Table I) indicate that under these conditions another (a third) path becomes evident. A possible mechanism for this path is equilibrium 1 followed by

$$[V\text{-}pyr]^{2+} + V_{aq}^{2+} \overset{fast}{\rightleftharpoons} V_2(pyr)^{4+} \qquad (6)$$

$$V_2(pyr)^{4+} \rightarrow lactic + 2V^{3+} \qquad (7)$$

with the organic ligand in $V_2(pyr)^{4+}$ possibly (but not necessarily) in bridging position.

The kinetic data for the reaction of V_{aq}^{2+} with phenylglyoxylic acid can be explained with the following reaction mechanism:

$$V_{aq}^{2+} + pgl \overset{fast}{\rightleftharpoons} \{V\text{-}\dot{p}gl\}^{2+} \qquad (1a)$$

$$\{V\text{-}pgl\}^{2+} \xrightarrow{slow} V(III) + pgl \qquad (2a)$$

$$2\dot{p}gl \xrightarrow{fast} dpt \qquad (3a)$$

where $\dot{p}gl$ is a free radical.

On the basis of this mechanism the observed rate constant $k^{(2)}_{obsd}$ is identified with $k_{2a}K_{1a}$. $K_{1a} = 4.0$ M^{-1}; therefore $k_{2a} = 6.5 \pm 0.7$ s^{-1}.

This mechanism only refers to the redox step, stage II, and it does not describe stage III. From Figure 4 it is clear that the spectra taken at time 1 s after mixing of the reactants and at infinite time correspond to V(III) species. Stage III, therefore, may be tentatively attributed to a reaction of a V(III) complex changing to a different V(III) complex of lower extinction coefficient, possibly through a rearrangement in the organic ligand.

It has long been recognized[8] that the rates of intramolecular electron transfer within binuclear complexes provide a powerful strategy for understanding fundamental aspects of the charge-transfer process across ligands. In the case of the so-called chemical mechanism, however, this intramolecular transfer can be further analyzed into two steps: transfer *to* and *from* the ligand. Reactions such as (3) and (2a) give direct information for transfer *to* the ligand. It could then be argued

that systems like the one reported here provide in some sense better "resolution". In addition, they allow direct measurement of their precursor equilibria and study of the competition between intramolecular and outer-sphere paths (eq 5). Both in intra- and intermolecular electron transfer across bridging ligands, the presence of the second metal ion, which acts as the sink for the electron, smooths out differences and gives similar rate laws, products, etc. In our system this leveling-off effect is missing. As a result systems differing only, e.g., by one electron, or by one functional group not participating directly in the reaction (e.g., methyl and phenyl groups in pyruvic and phenylglyoxylic acids, respectively), may show not merely a difference in rate and activation parameters, but a more dramatic difference in the rate law itself, the products obtained, the salient features of the mechanism, etc.

Comparing now pyruvic to phenylglyoxylic acid we observe that in the first intramolecular electron transfer is unambiguously distinguished from but is in competition with an outer-sphere path (eq 5). With phenylglyoxylic acid the outer-sphere path does not compete effectively anymore. The presence of the electron attracting phenyl ring presumably makes the metal-to-ligand transfer more effective. Related to this enhanced effectiveness is also the fact that only one phenylglyoxylic acid ligand is enough to attract the electron away from vanadous, whereas one pyruvato ligand cannot do the job. Substitution of one water molecule by one pyruvate ion in the coordination sphere of V(II) may increase the reducing ability of this ion and thus render the transfer of the electron to a second pyruvato ligand possible.

In reactions 3 and 2a the transfer of the electron causes labilization of the metal ion center, which facilitates the release (and subsequent dimerization) of the free radical. In this respect our system is the opposite to Taube's classical system $Cr^{II} \rightarrow Cr^{III}$, and it is perhaps relevant that in the reduction of pyruvic acid by chromous ion we did not observe[2] a free-radical path similar to the one observed with vanadous.

Acknowledgments. The authors wish to thank Mrs. E. Kissa-Meintany for laboratory assistance and the Secretary of the Chemistry Department, Mrs. K. Kaplany-Aravany, for secretarial assistance.

References and Notes

(1) Department of Chemistry, University of Athens, Navarinou 13a, Athens, Greece.
(2) J. Konstantatos, N. Katsaros, E. Vrachnou-Astra, and D. Katakis, *J. Am. Chem. Soc.*, **100**, 3128 (1978).
(3) N. Katsaros, E. Vrachnou-Astra, J. Konstantatos, and C. I. Stassinopoulou, *Tetrahedron Lett.*, in press.
(4) (a) H. J. Price, and H. Taube, *Inorg. Chem.*, **7**, 1 (1968); (b) Jean C. Chen and E. S. Gould, *J. Am. Chem. Soc.*, **95**, 5539 (1973).
(5) (a) F. A. Loewus, P. Ofner, H. F. Fisher, F. H. Westheimer, and B. Vennesland, *J. Biol. Chem.*, **202**, 699 (1953); (b) R. H. Abeles, R. F. Hutton, and F. H. Westheimer, *J. Am. Chem. Soc.*, **79**, 712 (1957); (c) R. F. Williams and T. C. Bruice, *ibid.*, **98**, 7752 (1976).
(6) E. Vrachnou-Astra, P. Sakellaridis, and D. Katakis, *J. Am. Chem. Soc.*, **92**, 811 (1970).
(7) (a) R. S. Stearns, and G. W. Wheland, *J. Am. Chem. Soc.*, **69**, 2025 (1947); (b) D. Katakis and E. Vrachnou-Astra, *Chim. Chron., New Ser.*, **1**, 225 (1972).
(8) (a) H. Taube and H. Myers, *J. Am. Chem. Soc.*, **76**, 2103 (1954); (b) S. Isied and H. Taube, *ibid.*, **95**, 8198 (1973); (c) A. Halm, *Acc. Chem. Res.*, **8**, 264 (1975).

The Mechanism of Asymmetric Homogeneous Hydrogenation. Rhodium(I) Complexes of Dehydroamino Acids Containing Asymmetric Ligands Related to Bis(1,2-diphenylphosphino)ethane[1]

John M. Brown* and Penny A. Chaloner

Contribution from the Dyson Perrins Laboratory, Oxford, OX1 3QY, England.
Received February 9, 1979

Abstract: The course of hydrogenation of dehydroamino acids by cationic rhodium complexes derived from bis(1,2-diphenylphosphino)ethane has been studied by phosphorus and carbon NMR. The parent complex reacts with hydrogen (1 atm) in methanol to form norbornane and the corresponding biphosphine rhodium solvate. Addition of (*Z*)-α-benzamidocinnamic acid causes displacement of solvent and formation of the corresponding 1:1 enamide complex. Comparable complexes, which may exist in diastereoisomeric forms, are obtained from chiral bis(1,2-diphenylphosphino)ethane derivatives. The ^{13}C NMR spectra of isotopically enriched enamide complexes demonstrate that the olefin and amide carbonyl groups bind to the metal, but that the carboxylate does not. (*E*)-Dehydroamino acids do not bind strongly to rhodium and isomerize readily with formation of the corresponding (*Z*)-enamide complex, but stable complexes are formed in the presence of triethylamine.

Introduction

Hydrogenation of prochiral olefins may generate a new asymmetric center. It was thus quickly recognized that complexes analogous to $(Ph_3P)_3RhCl$ had potential in asymmetric synthesis, and both chiral solvents[2] and a variety of asymmetric phosphines were employed in earlier work.[3-7] The use of chelating biphosphines proved to be very fruitful, especially in the asymmetric reduction of (*Z*)-dehydroamino acids.[8] While it would be inappropriate to give a comprehensive review here,[9] we note that the most effective catalysts are cationic complexes of chiral biphosphines (**1–5**) related to bis(1,2-diphenylphos-

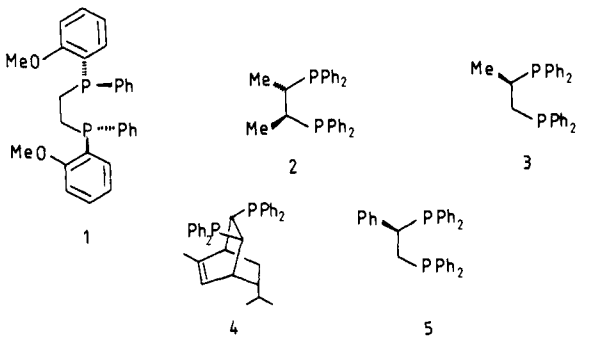

0002-7863/80/1502-3040$01.00/0